8th GRACM International Congress on Computational Mechanics
Volos, 12 July – 15 July 2015

ANALYSIS OF FRAMED STRUCTURES INCLUDING GENERALIZED WARPING EFFECTS

Evangelos J. Sapountzakis[1], Ioannis C. Dikaros[2], Amalia K. Argyridi[3] and Stergios K. Panos[4]

[1] Professor, School of Civil Engineering,
National Technical University,
Zografou Campus, GR–157 80, Athens, Greece
e-mail: cvsapoun@central.ntua.gr

[2] Doctoral Student, School of Civil Engineering,
National Technical University,
Zografou Campus, GR–157 80, Athens, Greece
e-mail: dikarosgiannis@gmail.com

[3] Doctoral Student, School of Civil Engineering,
National Technical University,
Zografou Campus, GR–157 80, Athens, Greece
e-mail: a.argyridi@gmail.com

[4] Army Corps of Engineers, Hellenic Army General Staff, Ministry of Defence,
Mesogeion Street 227-231, Holargos, PO BOX 15451, Greece
e-mail: s.k.panos@army.gr

Keywords: Nonuniform warping , stiffness matrix, composite, flexure, torsion, shear deformation

Abstract. *In this paper an advanced 20x20 stiffness matrix and the corresponding nodal load vector of a member of arbitrary composite cross section is developed taking into account shear lag effects due to both flexure and torsion. The composite member consists of materials in contact each of which can surround a finite number of inclusions. Nonuniform warping distributions are taken into account by employing four independent warping parameters multiplying a shear warping function in each direction and two torsional warping functions. Ten boundary value problems with respect to the kinematical components are formulated and solved employing a Boundary Element Method based technique. The aforementioned boundary value problems are formulated employing either an improved stress field arising from the correction of shear stress components or the stress field arising directly from displacement considerations. The warping functions and the geometric constants including the additional ones due to warping are evaluated employing a pure BEM approach. Numerical results are presented to illustrate the method and demonstrate its efficiency and accuracy. The deviations arising from the use of the advanced 20x20 stiffness matrix and the classical 12x12 or 14x14 ones employed in commercial software packages are illustrated through examples of great practical interest.*

1. INTRODUCTION

In engineering practice the analysis of spatial frames is frequently encountered. As far as their flexural behavior is concerned, the involved structural members of these frames are usually analyzed employing beam elements based on Euler-Bernoulli or Timoshenko beam theories. Both theories maintain the assumption that cross sections remain plane after deformation. Thus, the formulation remains simple; however it fails to capture "shear lag" phenomenon which is associated with a significant modification of normal stress distribution due to nonuniform shear warping [1,2] and has been reported long ago [3-5] in many structural members (e.g. beams of box-shaped cross sections, folded structural members, beams made of materials weak in shear). In up-to-date regulations, the significance of shear lag effect in flexure is recognized; however in order to simplify the analysis and permit the use of available conventional finite beam elements, the "effective breadth" concept [6-8] is recommended. This simplifying approach may fail to capture satisfactorily the actual structural behavior of the member, since the influence of shear lag phenomenon is not constant along the beam length, while apart from the geometrical configuration of the cross section it depends also on the type of loading [9,10].

In the present study an advanced 20x20 stiffness matrix and the corresponding nodal load vector of a member of arbitrary composite cross section is presented, capable of taking into account shear deformation and shear lag effects due to both flexure and torsion (the case of the 3-D beam element of arbitrary homogeneous cross section

is treated as a special one). The composite member consists of materials in contact each of which can surround a finite number of inclusions. Nonuniform warping distributions are taken into account by employing four independent warping parameters multiplying a shear warping function in each direction and two torsional warping functions. Ten boundary value problems with respect to the kinematical components are formulated and solved employing the Analog Equation Method [13], a Boundary Element Method based technique. It is worth here mentioning that the stress field arising from the above kinematical considerations leads to the violation of the longitudinal local equilibrium equation and the corresponding boundary condition [1,12] due to inaccurate representation of shear stresses (a similar discussion is made about the correction of torsional secondary shear stress distribution in [11]). The aforementioned boundary value problems are formulated employing either an improved stress field arising from the correction of shear stress components as this is presented in detail in [1] or the stress field originating directly from displacement considerations. In this study, the performance of both versions of the developed stiffness matrix is assessed. Warping functions and geometric constants including the additional ones due to warping are evaluated employing a pure BEM approach, i.e. only boundary discretization of the cross section is used.

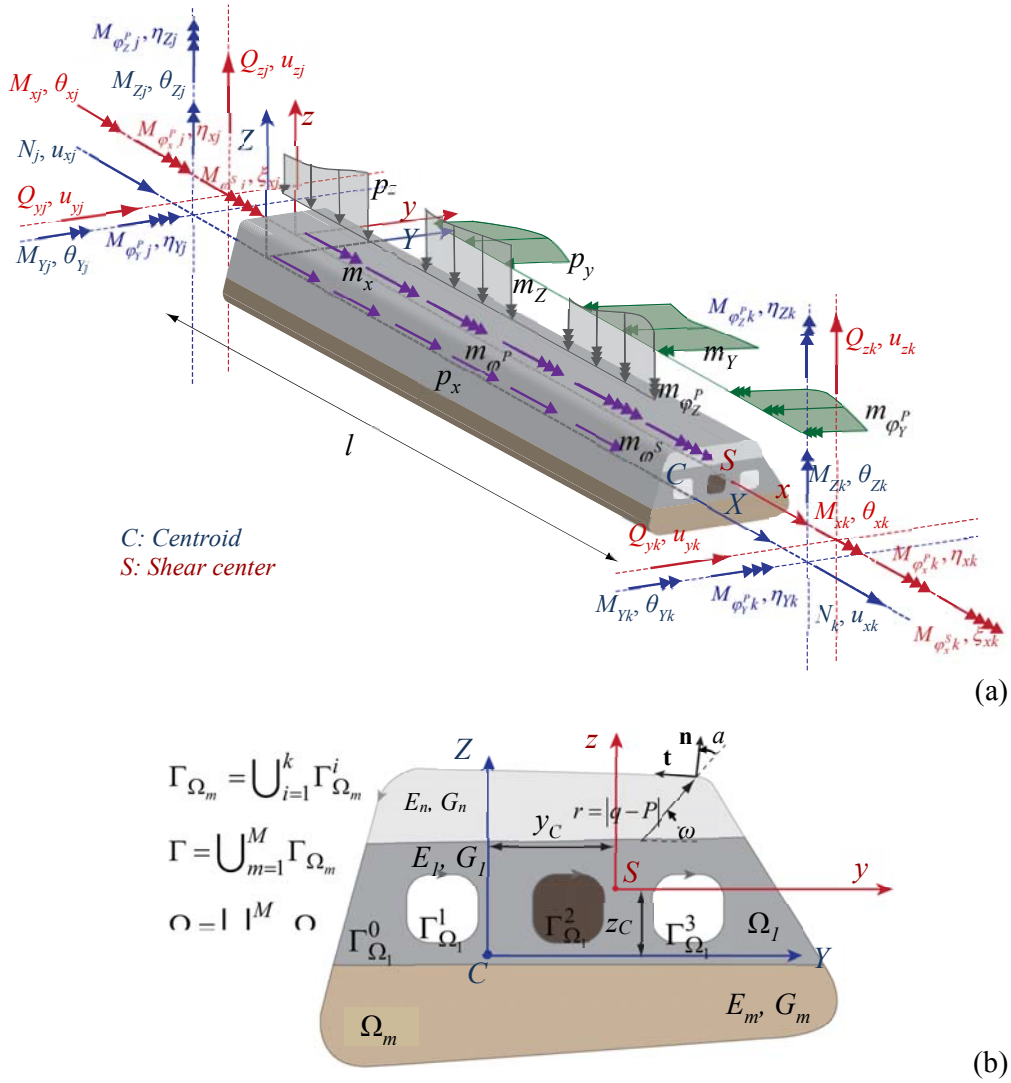

Figure 1. Prismatic beam element (a) with a composite cross section of arbitrary shape occupying the two dimensional region Ω (b).

2. STATEMENT OF THE PROBLEM

Consider a prismatic element of length l with an arbitrarily shaped composite cross section consisting of materials in contact, each of which can surround a finite number of inclusions, with modulus of elasticity E_m and shear modulus G_m, occupying the regions Ω_m ($m = 1,2,...,M$) of the yz plane (Figure 1b). The materials of these regions are assumed homogeneous, isotropic and linearly elastic. Let also the boundaries of the nonintersecting regions Ω_m be denoted by Γ_{Ω_m} ($m = 1,2,...,M$). These boundary curves are piecewise smooth, i.e. they may have a finite number of corners. In Figure 1 $CXYZ$ is the principal bending coordinate system through the cross section's centroid C, while y_C, z_C are its coordinates with respect to $Sxyz$ reference coordinate system through the cross section's shear center S. The beam element is subjected to the combined action of arbitrarily distributed or concentrated axial loading $p_x = p_x(X)$ along X direction, transverse loading $p_y = p_y(x)$ and $p_z = p_z(x)$ along the y, z directions, respectively, twisting moments $m_x = m_x(x)$ along x direction, bending moments $m_Y = m_Y(x)$, $m_Z = m_Z(x)$ along Y, Z directions, respectively, as well as to warping moments (bimoments) $m_{\varphi_x^P} = m_{\varphi_x^P}(x)$, $m_{\varphi_Y^P} = m_{\varphi_Y^P}(x)$, $m_{\varphi_Z^P} = m_{\varphi_Z^P}(x)$ and $m_{\varphi_x^S} = m_{\varphi_x^S}(x)$ (Figure 1a) [1]. The possible external loading of warping moments will be defined later (eqn (9)).

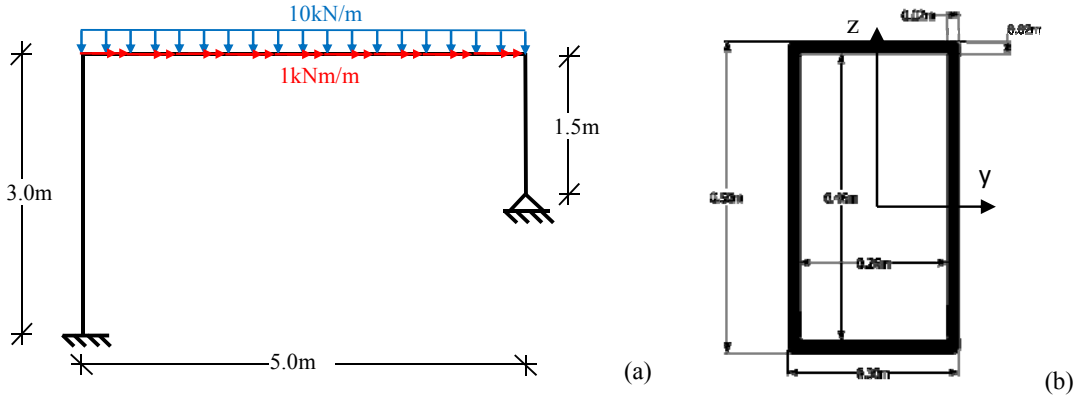

Figure 2. Geometry, boundary conditions, loading (a) and cross section of the frame (b) of the numerical example.

Table 1: Geometric constants of the cross section of the frame of the numerical example

Geometric constant	Value	Unit	Geometric constant	Value	Unit
A	3.03340 E-2	m^2	$I_{\varphi_x^P \varphi_x^P}$	8.94667 E-7	m^6
I_{yy}	1.01042 E-3	m^4	$I_{\varphi_y^P \varphi_y^P}$	2.85448 E-6	m^4
I_{zz}	4.49194 E-4	m^4	$I_{\varphi_z^P \varphi_z^P}$	1.48675 E-7	m^4
A_y	8.94076 E-3	m^2	$I_{\varphi_y^P \varphi_x^P}$	-7.57998 E-9	m^5
A_z	1.82493 E-2	m^2	$I_{\varphi_z^P \varphi_x^P}$	7.80773 E-10	m^5
I_t	9.80216 E-4	m^4	$I_{\varphi_x^S \varphi_y^P}$	-4.27323 E-10	m^5
C_s	9.03594E-7	m^6	$I_{\varphi_x^S \varphi_z^P}$	-5.82498 E-10	m^5
			$I_{\varphi_x^S \varphi_x^S}$	3.14321 E-8	m^6

Under the action of the aforementioned general loading and of possible restraints, the beam is leaded to flexure and/or torsion. Starting with the flexural behavior of the beam, the following remarks can be made. It is well-known that in case of non-constant bending moment distributions, shear stresses arise on horizontal sections of an infinitesimal beam element equilibrating the variation of *primary normal stresses* due to bending (σ_{xx}^P). Cauchy principle dictates that corresponding shear stresses arise on the plane of the cross section as well.

Contrary to Timoshenko beam theory prediction, these shear stresses have a nonuniform distribution over the domain of the

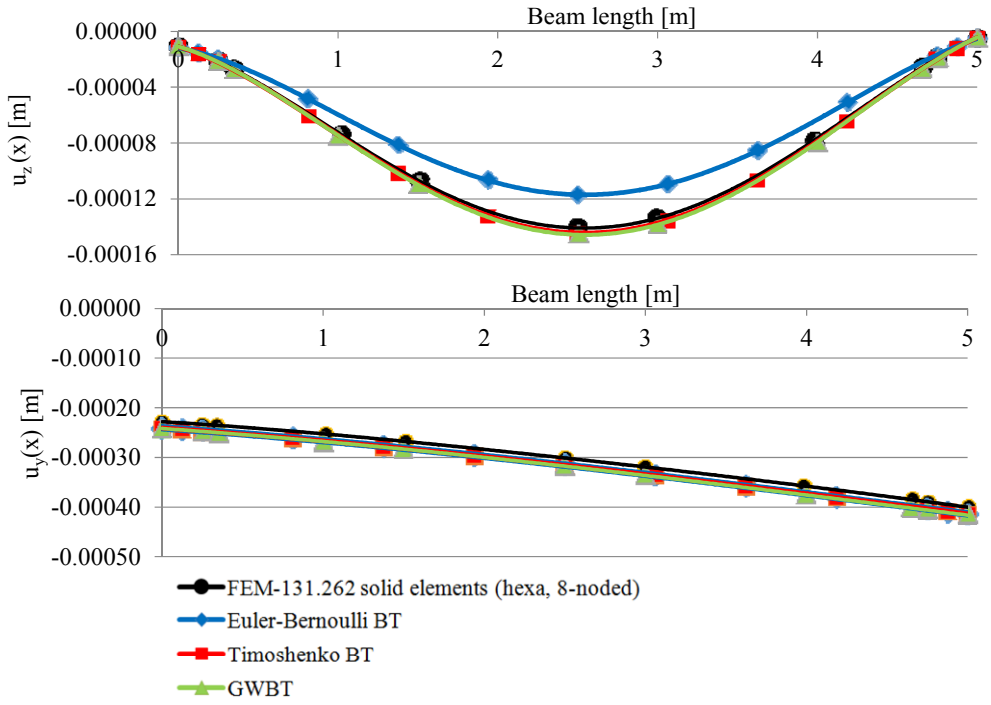

Figure 3. In plane (a) and out of plane (b) deflection of the beam of the frame of the numerical example.

cross section to satisfy local equilibrium and the requirement of vanishing tractions over the lateral surface. These shear stresses constitute the *primary or St.Venant shear stresses* (τ_{xz}^{P}, τ_{xy}^{P}) and lead the cross section to warp. Furthermore, due to the nonuniform character of this warping along the beam length a *secondary warping normal stress* distribution σ_{xx}^{S} is developed. This additional normal stress distribution is responsible for the well-known shear lag phenomenon and is taken into account by employing an independent warping parameter multiplying a corresponding warping function depending only on the cross sectional configuration [1]. The described nonuniform warping results in the development of *secondary shear stresses* τ_{xz}^{S}, τ_{xy}^{S} which equilibrate the variation of σ_{xx}^{S}. However, in an analogy with Timoshenko beam theory, the secondary shear stress distribution arising from the use of the aforementioned independent warping parameter fails to fulfill zero-traction condition on the lateral surface of the beam. In the present study, in order to remove this inconsistency a shear stress correction is performed modifying the stress field by adding an additional warping function to "correct" τ_{xz}^{S}, τ_{xy}^{S}. The above remarks are also valid for the problem of nonuniform torsion with STMDE [3,4]. In the present study, in order to take into account torsional shear lag effects as well, normal stress distribution due to secondary torsional warping φ_{S}^{S} [4] is also taken into account (*secondary normal stress* σ_{xx}^{S}). This distribution is equilibrated by corresponding *tertiary shear stresses* τ_{xz}^{T}, τ_{xy}^{T} which, similarly with the case of shear lag analysis in flexure, require a correction. In the present study this is achieved by adding an additional torsional warping function.

Within the context of the above considerations the generalized nodal displacement vector of the presented element in the local coordinate system, as shown in Figure 1a, can be written as

$$\left\{D^{i}\right\}=\left[u_{x}^{ij}\;\; u_{y}^{ij}\;\; u_{z}^{ij}\;\; \theta_{x}^{ij}\;\; \theta_{Y}^{ij}\;\; \theta_{Z}^{ij}\;\; \eta_{x}^{ij}\;\; \eta_{Y}^{ij}\;\; \eta_{Z}^{ij}\;\; \xi_{x}^{ij} \;\middle|\; u_{x}^{ik}\;\; u_{y}^{ik}\;\; u_{z}^{ik}\;\; \theta_{x}^{ik}\;\; \theta_{Y}^{ik}\;\; \theta_{Z}^{ik}\;\; \eta_{x}^{ik}\;\; \eta_{Y}^{ik}\;\; \eta_{Z}^{ik}\;\; \xi_{x}^{ik}\right]^{T} \quad (1)$$

and the respective nodal load vector as

$$\left\{F^{i}\right\}=\left[N^{ij}\;\; Q_{y}^{ij}\;\; Q_{z}^{ij}\;\; M_{x}^{ij}\;\; M_{Y}^{ij}\;\; M_{Z}^{ij}\;\; M_{\varphi_{x}^{P}}^{ij}\;\; M_{\varphi_{Y}^{P}}^{ij}\;\; M_{\varphi_{Z}^{P}}^{ij}\;\; M_{\varphi_{x}^{S}}^{ij} \;\middle|\; N^{ik}\right.$$

$$Q_y^{ik} \quad Q_z^{ik} \quad M_x^{ik} \quad M_Y^{ik} \quad M_Z^{ik} \quad M_{\varphi_x^P}^{ik} \quad M_{\varphi_Y^P}^{ik} \quad M_{\varphi_Z^P}^{ik} \quad M_{\varphi_x^S}^{ik} \Big]^T \tag{2}$$

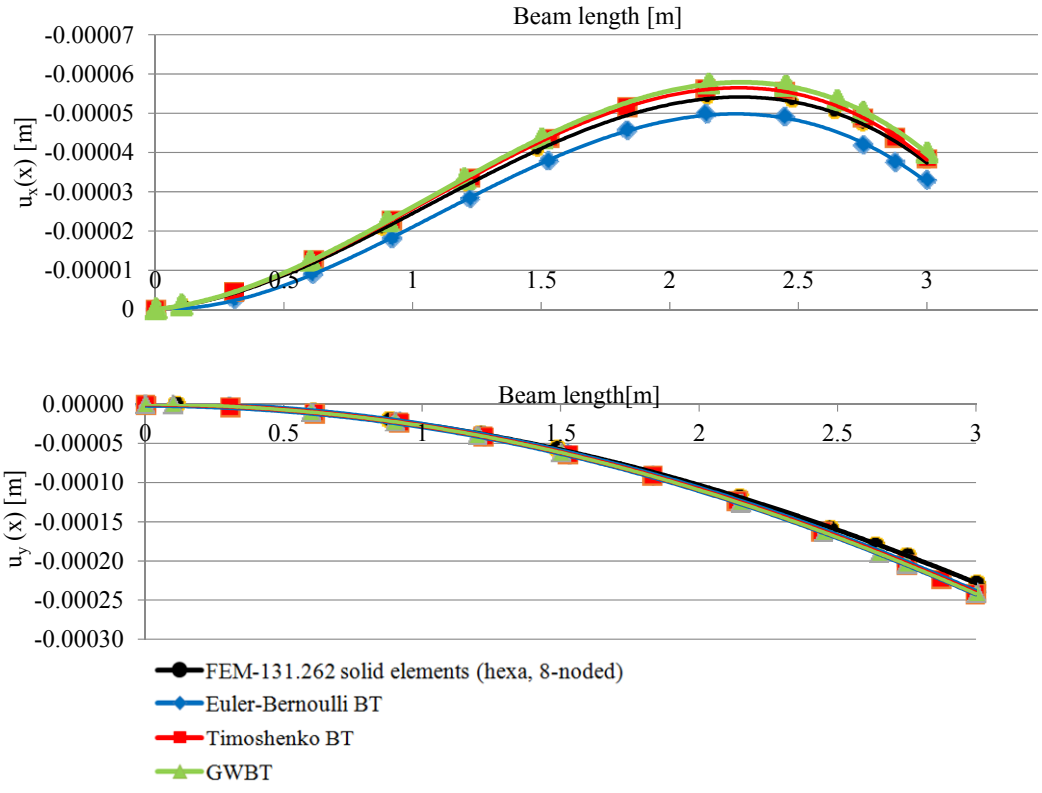

Figure 4. In plane (a) and out of plane (b) deflection of the left column of the numerical example.

In eqn(1) u_x is the "average" axial displacement of the cross section and u_y, u_z describe the transverse displacements of shear center S. Moreover, θ_Y, θ_Z are the angles of rotation due to bending along the centroidal Y, Z axes, respectively, while η_x, ξ_x are the independent warping parameters introduced to describe the nonuniform distribution of primary and secondary torsional warping and η_Y, η_Z the nonuniform distribution of primary warping due to shear. Index i denotes the i-th beam element, while indices j, k refer to each element end. In eqn (2) the stress resultants at the element ends as defined in [14], employing the definitions of geometric constants [14] are expressed in terms of the kinematical components as

$$N = E_{\text{ref}} A u_{x,x} \tag{3a}$$

$$Q_y^P = G_{\text{ref}} A_Y^P \gamma_Y^P \qquad Q_y^S = -G_{\text{ref}} \left(A_Y^S \gamma_Y^S + D_{\Phi_Z^S \Phi_x^S} \gamma_x^S + D_{\Phi_Z^S \Phi_x^T} \gamma_x^T \right) \tag{3b,c}$$

$$Q_z^P = G_{\text{ref}} A_Z^P \gamma_Z^P \qquad Q_z^S = -G_{\text{ref}} \left(A_Z^S \gamma_Z^S + D_{\Phi_Y^S \Phi_x^S} \gamma_x^S + D_{\Phi_Y^S \Phi_x^T} \gamma_x^T \right) \tag{3d,e}$$

$$M_x^P = G_{\text{ref}} I_x^P \theta_{x,x} \qquad M_x^S = -G_{\text{ref}} \left(I_x^S \gamma_x^S + D_{\Phi_Z^S \Phi_x^S} \gamma_Y^S + D_{\Phi_Y^S \Phi_x^S} \gamma_Z^S \right) \qquad M_x^T = G_{\text{ref}} \left(I_x^T \gamma_x^T + D_{\Phi_Z^S \Phi_x^T} \gamma_Y^S + D_{\Phi_Y^S \Phi_x^T} \gamma_Z^S \right) \tag{3f,g,h}$$

$$M_Y = E_{\text{ref}} I_{YY} \theta_{Y,x} \qquad M_Z = E_{\text{ref}} I_{ZZ} \theta_{Z,x} \tag{3i,j}$$

$$M_{\varphi_x^P} = E_{\text{ref}} \left(I_{\varphi_x^P \varphi_x^P} \eta_{x,x} + I_{\varphi_Y^P \varphi_x^P} \eta_{Y,x} + I_{\varphi_Z^P \varphi_x^P} \eta_{Z,x} \right) \qquad M_{\varphi_Y^P} = E_{\text{ref}} \left(I_{\varphi_Y^P \varphi_Y^P} \eta_{Y,x} + I_{\varphi_Y^P \varphi_x^P} \eta_{x,x} + I_{\varphi_Y^P \varphi_x^S} \xi_{x,x} \right) \tag{3k,l}$$

$$M_{\varphi_Z^P} = E_{\text{ref}} \left(I_{\varphi_Z^P \varphi_Z^P} \eta_{Z,x} + I_{\varphi_Z^P \varphi_x^P} \eta_{x,x} + I_{\varphi_Z^P \varphi_x^S} \xi_{x,x} \right) \qquad M_{\varphi_x^S} = E_{\text{ref}} \left(I_{\varphi_x^S \varphi_x^S} \xi_{x,x} + I_{\varphi_Y^P \varphi_x^S} \eta_{Y,x} + I_{\varphi_Z^P \varphi_x^S} \eta_{Z,x} \right) \tag{3m,n}$$

where $\gamma_Y^P = u_{y,x} - \theta_Z$, $\gamma_Y^S = \eta_Y - u_{y,x} + \theta_Z$, $\gamma_Z^P = u_{z,x} + \theta_Y$, $\gamma_Z^S = \eta_Z - u_{z,x} - \theta_Y$, $\gamma_x^P = \theta_{x,x}$, $\gamma_x^S = \eta_x - \theta_{x,x}$ and $\gamma_x^T = \xi_x - \eta_x + \theta_{x,x}$ are "average" shear strain quantities.

Finally the corresponding stress field expressions are given as

$$\left(\sigma_{xx}\right)_m = \underbrace{E_m\left[u_{,x} + \theta_{Y,x}Z - \theta_{Z,x}Y + \eta_{x,x}\left(\varphi_x^P\right)_m\right]}_{\text{primary}} + \underbrace{E_m\left[\eta_{Y,x}\left(\varphi_Y^P\right)_m + \eta_{Z,x}\left(\varphi_Z^P\right)_m + \xi_{x,x}\left(\varphi_x^S\right)_m\right]}_{\text{secondary}} \tag{4a}$$

$$\left(\tau_{xy}\right)_m = \underbrace{G_m\left\{\gamma_Z^P\left(\Phi_{Y,y}^P\right)_m + \gamma_Y^P\left(\Phi_{Z,y}^P\right)_m + \gamma_x^P\left[-z + \left(\varphi_{x,y}^P\right)_m\right]\right\}}_{\text{primary}} +$$

$$+ \underbrace{G_m\left\{\gamma_Z^S\left(\Phi_{Y,y}^S\right)_m + \gamma_Y^S\left(\Phi_{Z,y}^S\right)_m + \gamma_x^S\left(\Phi_{x,y}^S\right)_m\right\}}_{\text{secondary}} + \underbrace{G_m\left[\gamma_x^T\left(\Phi_{x,y}^T\right)_m\right]}_{\text{tertiary}} \tag{4b}$$

$$\left(\tau_{xz}\right)_m = \underbrace{G_m\left\{\gamma_Z^P\left(\Phi_{Y,z}^P\right)_m + \gamma_Y^P\left(\Phi_{Z,z}^P\right)_m + \gamma_x^P\left[y + \left(\varphi_{x,z}^P\right)_m\right]\right\}}_{\text{primary}} +$$

$$+ \underbrace{G_m\left[\gamma_Z^S\left(\Phi_{Y,z}^S\right)_m + \gamma_Y^S\left(\Phi_{Z,z}^S\right)_m + \gamma_x^S\left(\Phi_{x,z}^S\right)_m\right]}_{\text{secondary}} + \underbrace{G_m\left[\gamma_x^T\left(\Phi_{x,z}^T\right)_m\right]}_{\text{tertiary}} \tag{4c}$$

where

$$\Phi_x^S = \varphi_x^P + \varphi_x^S \qquad \Phi_x^T = \varphi_x^S + \varphi_x^T \qquad \Phi_Y^P = Z + \varphi_Y^P \qquad \Phi_Y^S = \varphi_Y^P + \varphi_Y^S \qquad \Phi_Z^P = Y + \varphi_Z^P \qquad \Phi_Z^S = \varphi_Z^P + \varphi_Z^S \tag{5a-f}$$

Warping functions due to shear Φ_Y^P, Φ_Z^P, Φ_Y^S, Φ_Z^S and due to torsion φ_x^P, Φ_x^S, Φ_x^T can be determined by corresponding two-dimensional boundary value problems exploiting the longitudinal local equilibrium equation and the associated boundary condition, which is given in [14].

The nodal displacement and load vectors given in eqs (1), (2) are related with the 20x20 local stiffness matrix of the spatial beam element written as

$$\left[k^i\right] = \begin{bmatrix}
k_{11}^i & & & & & & & & & & & & & & & & & & & \\
0 & k_{22}^i & & & & & & & & & & & & & & & & & & \\
0 & k_{32}^i & k_{33}^i & & & & & & & & & & & & & & & & & \\
0 & k_{42}^i & k_{43}^i & k_{44}^i & & & & & & & & & & & & & & & & \\
0 & k_{52}^i & k_{53}^i & k_{44}^i & k_{55}^i & & & & & & & & & & & & & & & \\
0 & k_{62}^i & k_{63}^i & k_{64}^i & k_{65}^i & k_{66}^i & & & & & & & & & & & & & & \\
0 & k_{72}^i & k_{73}^i & k_{74}^i & k_{75}^i & k_{76}^i & k_{77}^i & & & & & & & & & & & & & \\
0 & k_{82}^i & k_{83}^i & k_{84}^i & k_{85}^i & k_{86}^i & k_{87}^i & k_{88}^i & & & & & & & & & & & & \\
0 & k_{92}^i & k_{93}^i & k_{94}^i & k_{95}^i & k_{96}^i & k_{97}^i & k_{98}^i & k_{99}^i & & & & & & & & & & & \\
0 & k_{10,2}^i & k_{10,3}^i & k_{10,4}^i & k_{10,5}^i & k_{10,6}^i & k_{10,7}^i & k_{10,8}^i & k_{10,9}^i & k_{10,10}^i & & & & & & & & & & \\
k_{11,1}^i & 0 & 0 & 0 & 0 & 0 & 0 & 0 & 0 & 0 & k_{11,11}^i & & & & & & & & & \\
0 & k_{12,2}^i & k_{12,3}^i & k_{12,4}^i & k_{12,5}^i & k_{12,6}^i & k_{12,7}^i & k_{12,8}^i & k_{12,9}^i & k_{12,10}^i & 0 & k_{12,12}^i & & & & & & & & \\
0 & k_{13,2}^i & k_{13,3}^i & k_{13,4}^i & k_{13,5}^i & k_{13,6}^i & k_{13,7}^i & k_{13,8}^i & k_{13,9}^i & k_{13,10}^i & 0 & k_{13,12}^i & k_{13,13}^i & & & & & & & \\
0 & k_{14,2}^i & k_{14,3}^i & k_{14,4}^i & k_{14,5}^i & k_{14,6}^i & k_{14,7}^i & k_{14,8}^i & k_{14,9}^i & k_{14,10}^i & 0 & k_{14,12}^i & k_{14,13}^i & k_{14,14}^i & & & & & & \\
0 & k_{152}^i & k_{15,3}^i & k_{15,4}^i & k_{15,5}^i & k_{15,6}^i & k_{15,7}^i & k_{15,8}^i & k_{15,9}^i & k_{15,10}^i & 0 & k_{15,12}^i & k_{15,13}^i & k_{15,14}^i & k_{15,15}^i & & & & & \\
0 & k_{16,2}^i & k_{16,3}^i & k_{16,4}^i & k_{16,5}^i & k_{16,6}^i & k_{16,7}^i & k_{16,8}^i & k_{16,9}^i & k_{16,10}^i & 0 & k_{16,12}^i & k_{16,13}^i & k_{16,14}^i & k_{16,15}^i & k_{16,16}^i & & & & \\
0 & k_{17,2}^i & k_{17,3}^i & k_{17,4}^i & k_{17,5}^i & k_{17,6}^i & k_{17,7}^i & k_{17,8}^i & k_{17,9}^i & k_{17,10}^i & 0 & k_{17,12}^i & k_{17,13}^i & k_{17,14}^i & k_{17,15}^i & k_{17,16}^i & k_{17,17}^i & & & \\
0 & k_{18,2}^i & k_{18,3}^i & k_{18,4}^i & k_{18,5}^i & k_{18,6}^i & k_{18,7}^i & k_{18,8}^i & k_{18,9}^i & k_{18,10}^i & 0 & k_{18,12}^i & k_{18,13}^i & k_{18,14}^i & k_{18,15}^i & k_{18,16}^i & k_{18,17}^i & k_{18,18}^i & & \\
0 & k_{19,2}^i & k_{19,3}^i & k_{19,4}^i & k_{19,5}^i & k_{19,6}^i & k_{19,7}^i & k_{19,8}^i & k_{19,9}^i & k_{19,10}^i & 0 & k_{19,12}^i & k_{19,13}^i & k_{19,14}^i & k_{19,15}^i & k_{19,16}^i & k_{19,17}^i & k_{19,18}^i & k_{19,19}^i & \\
0 & k_{20,2}^i & k_{20,3}^i & k_{20,4}^i & k_{20,5}^i & k_{20,6}^i & k_{20,7}^i & k_{20,8}^i & k_{20,9}^i & k_{20,10}^i & 0 & k_{20,12}^i & k_{20,13}^i & k_{20,14}^i & k_{20,15}^i & k_{16,16}^i & k_{20,17}^i & k_{20,18}^i & k_{20,19}^i & k_{20,20}^i
\end{bmatrix} \tag{6}$$

sym.

where the k_{jk}^i ($j,k = 1,2,...,20$) coefficients are established by expressions (3) obtained by solving the following system of differential equations [1]

$$-N_{,x} = p_x \tag{7a}$$

$$-\left(Q_y^P + Q_y^S\right)_{,x} = p_y \qquad -\left(Q_z^P + Q_z^S\right)_{,x} = p_z \tag{7b,c}$$

$$-\left(M_x^P + M_x^S + M_x^T\right)_{,x} = m_x \tag{7d}$$

$$-M_{Y,x}-\left(Q_z^P+Q_z^S\right)=m_Y \qquad -M_{Z,x}-\left(Q_y^P+Q_y^S\right)=m_Z \tag{7e,f}$$

$$-M_{\varphi_x^P,x}-M_x^S-M_x^T=m_{\varphi_x^P} \qquad -M_{\varphi_Y^P,x}-Q_z^S=m_{\varphi_Y^P} \tag{7g,h}$$

$$-M_{\varphi_Z^P,x}-Q_y^S=m_{\varphi_Z^P} \qquad -M_{\varphi_x^S,x}-M_x^T=m_{\varphi_x^S} \tag{7i,j}$$

subjected to the corresponding boundary conditions, which are given as

$$a_1u_x+\alpha_2N=\alpha_3 \tag{8a}$$

$$\beta_1u_y+\beta_2Q_y=\beta_3 \qquad \gamma_1u_z+\gamma_2Q_z=\gamma_3 \tag{8b,c}$$

$$\overline{\beta}_1\theta_Z+\overline{\beta}_2M_Z=\overline{\beta}_3 \qquad \overline{\gamma}_1\theta_Y+\overline{\gamma}_2M_Y=\overline{\gamma}_3 \tag{8d,e}$$

$$\tilde{\beta}_1\eta_Z+\tilde{\beta}_2M_{\varphi_Z^P}=\tilde{\beta}_3 \qquad \tilde{\gamma}_1\eta_Y+\tilde{\gamma}_2M_{\varphi_Y^P}=\tilde{\gamma}_3 \tag{8f,g}$$

$$\delta_1\theta_x+\delta_2M_x=\delta_3 \qquad \overline{\delta}_1\eta_x+\overline{\delta}_2M_{\varphi_x^P}=\overline{\delta}_3 \qquad \tilde{\delta}_1\xi_x+\tilde{\delta}_2M_{\varphi_x^S}=\tilde{\delta}_3 \tag{8h,i,j}$$

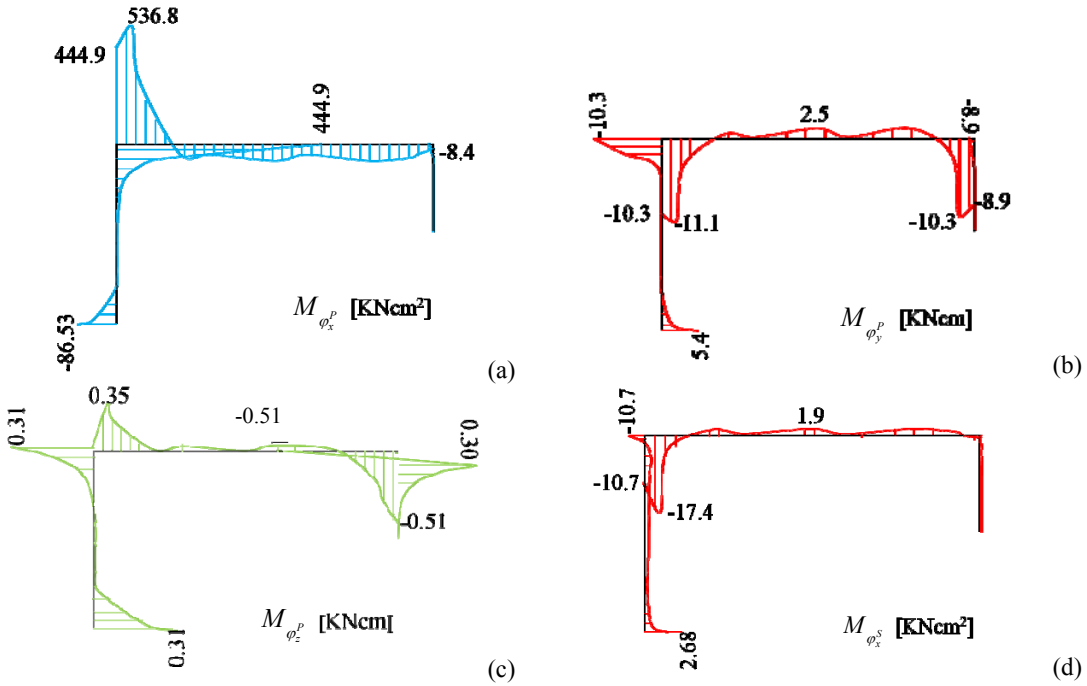

Figure 5. Distribution of $M_{\varphi_x^P}$ (a), $M_{\varphi_y^P}$ (b), $M_{\varphi_z^P}$ (c) and $M_{\varphi_x^S}$ (d) warping bimoments of the frame of the numerical example.

setting the external loading quantities equal to zero and applying appropriate values to functions $\alpha_i,\ \beta_i,\ \overline{\beta}_i,\tilde{\beta}_i,\gamma_i,\ \overline{\gamma}_i,\ \tilde{\gamma}_i,\delta_i,\overline{\delta}_i,\tilde{\delta}_i$ $(i=1,2,3)$ (e.g. for a unitary u_y displacement at $x=0$ it is: $\alpha_1=\beta_1=\overline{\beta}_1=\tilde{\beta}_1=\gamma_1=\overline{\gamma}_1=\tilde{\gamma}_1=\delta_1=\overline{\delta}_1=\tilde{\delta}_1=1,\ \ \beta_3=1,\ \ \alpha_2=\alpha_3=\beta_2=\overline{\beta}_2=\overline{\beta}_3=\tilde{\beta}_2=\tilde{\beta}_3=\gamma_2=\overline{\gamma}_3=\tilde{\gamma}_2=\tilde{\gamma}_3=\delta_2=\delta_3=\overline{\delta}_2=\overline{\delta}_3=\tilde{\delta}_2=\tilde{\delta}_3=0$). In eqs (7) the externally applied warping moments m_i $(i=\varphi_x^P,\varphi_Y^P,\varphi_Z^P,\varphi_x^S)$ are related to the component t_x of the traction vector applied on the lateral surface of the beam as

$$m_i(x)=\int_\Gamma t_x(i)\,\mathrm{d}s,\quad i=\varphi_x^P,\varphi_Y^P,\varphi_Z^P,\varphi_x^S \tag{9}$$

According to the nodal load vector, assuming that the span of the beam is subjected to arbitrarily concentrated or distributed axial loading p_x, transverse loading p_y, p_z, twisting moment m_x, bending moments m_Y, m_Z, as well as warping moments $m_{\varphi_x^P}$, $m_{\varphi_Y^P}$, $m_{\varphi_Z^P}$, $m_{\varphi_x^S}$, the evaluation of the elements of $\{F^i\}$ is accomplished establishing again the solution of the boundary value problems (7), (8) for appropriate values of

$\alpha_i,\ \beta_i,\ \overline{\beta}_i, \tilde{\beta}_i, \gamma_i,\ \overline{\gamma}_i,\ \tilde{\gamma}_i, \delta_i, \overline{\delta}_i, \tilde{\delta}_i \quad (i=1,2,3)$ and more specifically, for $\alpha_1=\beta_1=\overline{\beta}_1=\tilde{\beta}_1=\gamma_1=\overline{\gamma}_1=\tilde{\gamma}_1=\delta_1=\overline{\delta}_1=\tilde{\delta}_1=1$, $\alpha_2=\alpha_3=\beta_2=\beta_3=\overline{\beta}_2=\overline{\beta}_3=\tilde{\beta}_2=\tilde{\beta}_3=\gamma_2=\overline{\gamma}_3=\tilde{\gamma}_2=\tilde{\gamma}_3=\delta_2=\delta_3=\overline{\delta}_2=\overline{\delta}_3=\tilde{\delta}_2=\tilde{\delta}_3=0$ at $x=0,l$.

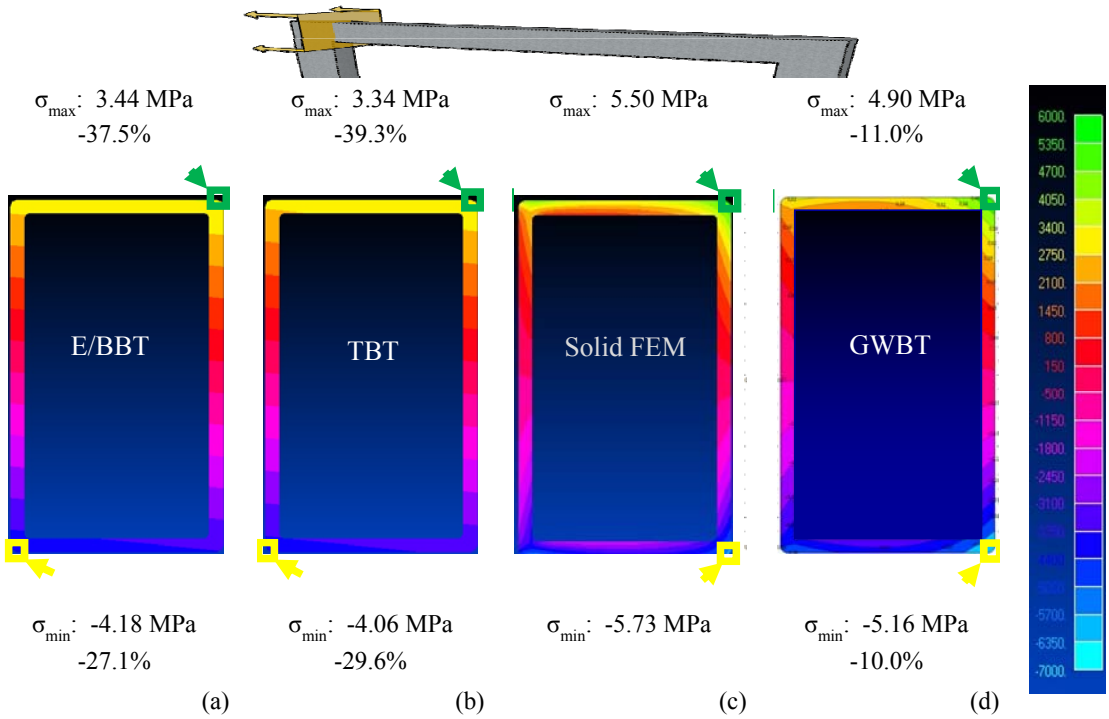

Figure 6. Distribution of normal stresses σ_{xx} at the left end of the beam of the frame of the numerical example, according to E/BBT [15,16] (a), TBT [15,16] (b), Solid FEM [15,16] (c) and GWBT (d) solutions along with maximum and minimum values and their discrepancies with respect to Solid FEM solution.

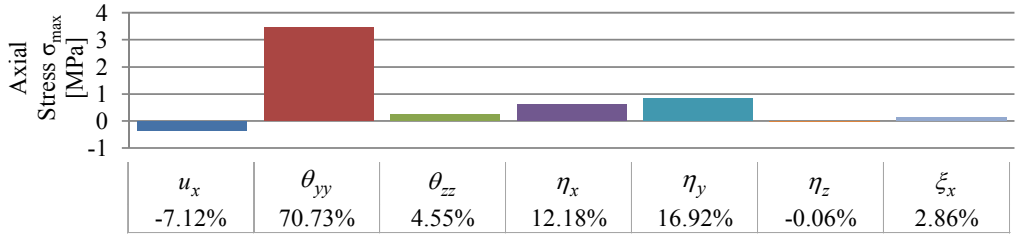

Figure 7. Contribution of each kinematical component to the maximum normal stress σ_{xx} at the left end of the beam (σ_{max}= 4.90 MPa) according to GWBT

3 NUMERICAL SOLUTION

According to the precedent analysis, the nonuniform shear problem of composite beams reduces in establishing the components $u(x)$, $v(x)$, $w(x)$, $\theta_x(x)$, $\theta_Y(x)$, $\theta_Z(x)$, $\eta_x(x)$, $\eta_Y(x)$, $\eta_Z(x)$ and $\xi_x(x)$ having continuous derivatives up to the second order with respect to x at the interval $(0,l)$ and up to the first order at $x=0,l$, satisfying the boundary value problem described by the coupled governing differential equations of equilibrium (eqs (7)) along the beam and the boundary conditions (eqs (8)) at the beam ends $x=0,l$. Equations (7), (8) are solved using the Analog Equation Method (AEM) [13], a BEM based method. Application of the boundary element technique yields a system of linear coupled algebraic equations which can

be solved without any difficulty. The geometric constants of the cross section [1,2] are evaluated employing a pure BEM approach, i.e. only boundary discretization of the cross section is used.

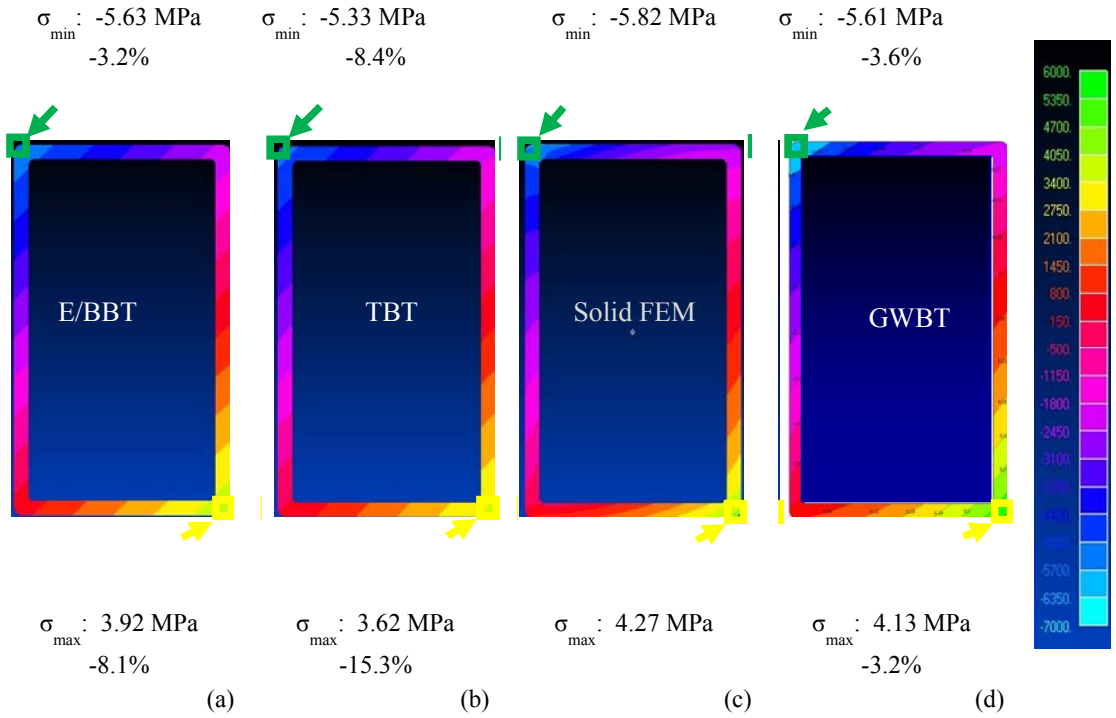

Figure 8. Distribution of normal stresses σ_{xx} at the fixed end of the left column of the frame of the numerical example, according to E/BBT [15,16] (a), TBT [15,16] (b), Solid FEM [15,16] (c) and GWBT (d) solutions along with maximum and minimum values and their discrepancies with respect to Solid FEM solution.

4. NUMERICAL EXAMPLE

In this example, the flexural-torsional response of a rectangular cross section (RHS500x300x20, Figure 2b) steel frame ($E = 210\ GPa$, $\nu = 0.3$) has been examined. The frame consists of two columns and one beam. The left column has length $3.0m$ and is fixed while the right one has length $1.5m$ and is simply supported (Figure 2a). The beam's length is $5.0m$ and is subjected to the combined action with a uniformly distributed transverse load of $10\ KN/m$ and a uniformly distributed torsional load of $1KNm/m$ as shown in Figure 2a.

More specifically, the boundary value problem of eqs (7), (8) has been solved to obtain the response of Generalized Warping Beam Theory (GWBT). For comparison reasons Euler Bernoulli Beam Theory (E/BBT [15,16]), Timoshenko Beam Theory (TBT [15,16]) and Solid (3-D hexahedral elements extruded by quadrilateral surfaces) FEM [15,16] models have been analyzed. In the Solid FEM model a few rigid diaphragms at appropriate positions have been used, corresponding to the assumption employed in the proposed method that the cross section maintains its shape at the transverse directions during deformation (no distortion effects). In GWBT, E/BBT and TBT solution 30 elements have been employed, while 131.262 solid elements have been employed for the Solid FEM model. In order to be able the comparison of stresses between the beam and 3d Solid models the joints between the columns and the beam have been modeled employing beam elements with geometric constants 500 times larger than the cross section of the frame.

Table 1 shows the geometric constants of the cross section of the frame. Figures 3 and 4 illustrate the in plane and out of plane deflection of the beam and the left column of the frame. Comparing the kinematic components it is concluded that TBT and GWBT results are very close to Solid FEM solution. That doesn't hold for E/BBT results. Figure 5 presents the distribution of $M_{\varphi_x^P}$, $M_{\varphi_y^P}$, $M_{\varphi_z^P}$ and $M_{\varphi_x^S}$ warping bimoments showing that their values are very small away from supports and nodes, while getting closer to fixed supports (restraint of kinematic components $\eta_x, \eta_y, \eta_z, \xi_{xj}$ or nodes (member unions), they increase exponentially.

Figures 6 and 8 show the distribution of normal stresses σ_{xx} according to E/BBT, TBT, Solid FEM and GWBT solutions, along with maximum and minimum values and their discrepancies with respect to Solid FEM

solution, at the left end of the beam and at the fixed support of the frame. Figure 7 presents the contribution of each kinematical component of the GWBT solution to the maximum normal stress. E/BBT and TBT, by adopting the assumption of plane cross section, present axial stress distribution contours which are consisted of straight lines. They cannot approximate axial stress distribution as obtained by the most accurate Solid FEM. On the contrary, by taking into account torsional and flexural warping through GWBT, the resulting axial stress distribution has significant convergence. Furthermore, E/BBT and TBT discrepancies with respect to Solid FEM solution in terms of maximum normal stresses is up to 37%. and 39% respectively. On the contrary, GWBT maximum discrepancy with respect to Solid FEM is 11%.

ACKNOWLEDGEMENTS

This research has been co-financed by the European Union (European SocialFund - ESF) and Greek national funds through the Operational Program "Education and Lifelong Learning" of the National Strategic ReferenceFramework (NSRF) - Research Funding Program: THALES: Reinforcement of the interdisciplinary and/or inter-institutional research and innovation.

REFERENCES

1. Dikaros I.C., Sapountzakis E.J. Generalized Warping Analysis of Composite Beams of Arbitrary Cross Section by BEM Part I: Theoretical Considerations and Numerical Implementation. *Journal of Engineering Mechanics ASCE*, in press, DOI: 10.1061/(ASCE)EM.1943-7889.0000775.
2. Dikaros I.C., Sapountzakis E.J. Generalized Warping Analysis of Composite Beams of Arbitrary Cross Section by BEM Part II: Numerical Applications. *Journal of Engineering Mechanics ASCE*, in press, DOI: 10.1061/(ASCE)EM.1943-7889.0000776.
3. Reissner E. Analysis of shear lag in box beams by the principle of minimum potential energy. *Q. Appl. Math.* 1946; 41:268-78.
4. Malcolm D.J., Redwood R.G. Shear lag in stiffened box-girders. *J. Struct. Div. ASCE* 1970; 96(ST7):1403-15.
5. Moffatt K.R., Dowling P.J. Shear lag in steel box-girder bridges. *Struct. Engineer* 1975; 53:439-48.
6. Eurocode 3: Design of Steel Structures – Part 1.5: Plated Structural Elements, European Committee for Standardization, prEN 1993-1-5: 2004.
7. Eurocode 4: Design of Composite Steel and Concrete Structures – Part 1.1: General Rules and Rules for Buildings, European Committee for Standardization, prEN 1994-1-1: 2004.
8. Eurocode 4: Design of Composite Steel and Concrete Structures – Part 2: General Rules and Rules for Bridges, European Committee for Standardization, prEN 1994-2: 2004.
9. Ie C.A., Kosmatka J.B. On the Analysis of Prismatic Beams Using First-Order Warping Functions. *International Journal of Solids and Structures* 1992; 29(7):879-891.
10. Katsikadelis J.T., Sapountzakis E.J. A Realistic Estimation of the Effective Breadth of Ribbed Plates. *International Journal of Solids and Structures* 2002; 39:897-910.
11. Tsipiras V.J., Sapountzakis E.J. Secondary Torsional Moment Deformation Effect in Inelastic Nonuniform Torsion of Bars of Doubly Symmetric Cross Section by BEM. *International Journal of Non-linear Mechanics* 2012; 47, 68-84.
12. Genoese A., Genoese A., Bilotta A., Garcea G. A Mixed Beam Model with Non-Uniform Warpings Derived from the Saint Venànt Rod. *Computers and Structures* 2013; 121:87-98.
13. Katsikadelis J.T. The Analog Equation Method. A Boundary – only Integral Equation Method for Nonlinear Static and Dynamic Problems in General Bodies. *Theoretical and Applied Mechanics* 2002; 27:13-38.
14. Sapountzakis E.J.and Dikaros I.C. "Advanced 3–D Beam Element of Arbitrary Composite Cross Section Including Generalized Warping Effects", International Journal for Numerical Methods in Engineering,DOI: 10.1002/nme.4849, 2015.
15. Siemens PLM Software Inc. *NX Nastran User's Guide*; 2008.
16. FEMAP for Windows. *Finite element modeling and post-processing software. Help System Index*, Version 11; 2013.